Scaling of the durations of chaotic transients in windows of attracting periodicity

Joeri Jacobs and Edward Ott*
Institute for Plasma Research and Department of Physics, University of Maryland, College Park, Maryland 20742

Brian R. Hunt†
Institute for Physical Science and Technology and Department of Mathematics, University of Maryland, College Park, Maryland 20742
(Received 7 July 1997)

As a bifurcation parameter μ is varied it is common for chaotic systems to display windows of width $\Delta\mu$ in which there is stable periodic behavior. In this paper we examine the dependence of the transient time τ of a periodic window (i.e., the typical time an initial condition wanders around chaotically before settling into periodic behavior) on the size of the periodic window $\Delta\mu$. We argue and numerically verify that for one-dimensional maps with a quadratic extremum $1/\tau \sim (\Delta\mu)^{1/2}$ and we find an asymptotic universal form for the parameter dependence of τ within individual high-period windows. For two-dimensional maps, we conjecture that for small windows the scaling changes to $1/\tau \sim (\Delta\mu)^{d-1/2}$, where d is a fractal dimension associated with a typical attractor for chaotic parameter values near the considered periodic windows.
[S1063-651X(97)01412-8]

PACS number(s): 05.45.+b

I. INTRODUCTION

Bifurcation diagrams, a pictorial way of displaying the dependence of trajectories of nonlinear dynamical systems on a system parameter, have been studied extensively [1]. As the system parameter is varied, one often observes a structure of chaotic parameter values and ''windows of periodicity.'' By a ''window of periodicity'' we mean an interval of system parameter values for which an arbitrary initial condition will be attracted to a periodic orbit. (Perhaps the most well-known example of this phenomenon is the period-three window of the logistic map.) Typically, as the parameter value varies, a window is initiated by a saddle-node bifuraction, at which a period-n attracting orbit is born. This orbit undergoes a period-doubling cascade as the system parameter is increased, becomes a small n-piece chaotic attractor, and finally the window terminates via a crisis [2]. Complementary to these periodic parameter values are the chaotic ones for which two initial conditions that were arbitrarily close initially exponentially diverge from each other and never settle into periodic behavior. It has been shown that for typical chaotic dynamical systems, the periodic windows are dense [3] and the set of chaotic parameter values has a strictly positive measure [4].

Furthermore, it has been shown that the global structure of these windows shows universal behavior in the sense that essential features are independent of the size of the window or the particular dynamical system under consideration. For example, if one compares the distance in parameter space from the saddle node to the crisis to the distance from the saddle node to the first period doubling, then, according to Ref. [5], this ratio approaches 9/4 for typical high-period windows.

Despite the asymptotic attracting periodic behavior in the windows, a randomly picked initial condition can often be seen to wander chaotically for some time before settling into periodic behavior. As a matter of fact, for any parameter value in a periodic window there will be a chaotic nonattracting invariant fractal set supporting trajectories that never land on the periodic attractor. Therefore, if a randomly picked initial condition happens to lie close to this set, its orbit will follow the chaotic behavior on the chaotic set for a while before being attracted to the periodic orbit. This has been called transient chaos [1,2,6]. The ''transient time,'' i.e., the average time an orbit will move around chaotically before exhibiting periodic behavior, will be studied in this paper. In particular, we will show that, for a one-dimensional chaotic map with a quadratic extremum, this transient time scales with the ''size of the window,'' the difference in parameter value between the final crisis and the saddle-node bifurcation. The reason for this scaling lies in the universal structure of the windows.

In Sec. II we argue that the transient time scales with the size of the window as

$$\frac{1}{\tau} \sim \Delta\mu^{1/2}. \tag{1}$$

We numerically verify the scaling law (1) in Sec. III for the quadratic map

$$x \to \mu - x^2 \tag{2}$$

and for the cubic map

$$x \to x^3 - 3\mu x. \tag{3}$$

In Sec. IV we show that the variation of the transient time as the parameter varies within a window follows a universal curve. In particular, for most windows, the largest transient

*Also at Department of Electrical Engineering and Institute for Systems Research, University of Maryland, College Park, MD 20742.
†FAX: (301) 314 9363. Electronic address: bhunt@ipst.umd.edu

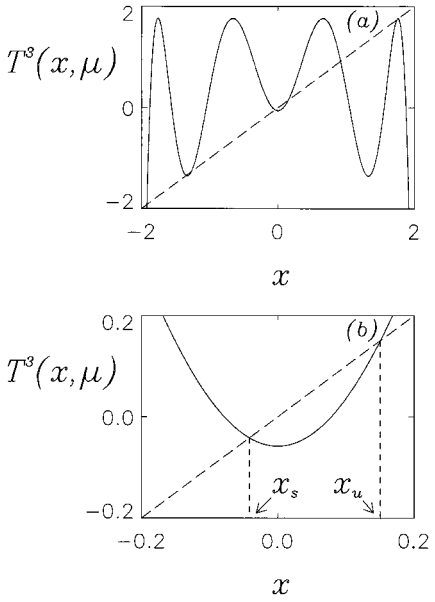

FIG. 1. (a) 3-times iterated map $T^3(x,\mu)$ for $T(x,\mu)=\mu-x^2$ and $\mu=1.765$, which is in the period-three window. (b) Blowup of $T^3(x,\mu)$ near the critical point $x=0$ and definition of the immediate basin $[-x_u,x_u]$.

time is approximately four times as large as the smallest one. Therefore, one can scale transient times of different windows and different maps to the universal curve by looking at corresponding parameter values in the different windows, for example, the value halfway between the saddle node and the crisis.

In Sec. V we consider window transient-time scaling for two-dimensional maps. We find that the Jacobian determinant of the map (i.e., the area contraction rate) must be very small for the one-dimensional scaling to hold. As this very small value is exceeded, we find a crossover to another type of scaling. In this latter regime we present a heuristic argument for the conjecture that

$$\frac{1}{\tau}\sim\Delta\mu^{d-1/2}, \tag{4}$$

where d is a fractal dimension associated with a typical chaotic attractor for chaotic parameter values near the periodic windows under consideration. We compare our conjecture for two-dimensional maps with numerical results for the Hénon map in Sec. VI.

II. THEORY FOR THE SCALING LAW

Consider the quadratic map

$$x\rightarrow T(x,\mu)=\mu-x^2. \tag{5}$$

Orbits in the x interval $[T^2(0,\mu),T(0,\mu)]=[\mu-\mu^2,\mu]$ remain in that interval for all time, and we are interested in the attractors and nonattracting invariant sets in that interval. In order to define more precisely what we mean by ''settling into periodic behavior,'' consider Fig. 1(a), which shows the third iterate of the map (5) for $\mu=1.765$, which lies in a period-three window. Now consider the blowup of the map $T^3(x,\mu)$ near $x=0$, shown in Fig. 1(b). Let $x_s(x_u)$ denote the element of the stable (unstable) period-three orbit closest to $x=0$. One can see that as soon as an itinerary falls in the interval $[-x_u,x_u]$, it will move monotonically toward x_s under the application of the map $T^3(x,\mu)$ and will converge to that point asymptotically. Therefore, we call the interval $[-x_u,x_u]$ the *immediate basin*.

The universal structure of large-n period-n windows as described before is a consequence of the universal behavior of the n-times iterated map for a period-n window near one of its stable periodic points. More precisely, for general one-dimensional maps with a quadratic extremum and for typical large n windows it can be shown that under a proper linear rescaling of x and μ the nth iterated map is well approximated by the canonical one-dimensional quadratic map

$$v_{n+1}=v_n+v_n^2-\nu, \tag{6}$$

where to lowest order ν is a linear function of μ. For this canonical form the original saddle-node bifurcation and the first period doubling occur at $\nu=0$ and $\nu=1$, respectively.

We define a *reduced Lyapunov number* for a twice differentiable one-dimensional map with a single quadratic maximum as follows. Let $S_1,S_2,\ldots,S_n$ be the widths of the immediate basins near each of the points of the period-n orbit, with S_1 including the critical point. Then we have that

$$S_2\cong KS_1^2, \tag{7}$$

where K is a constant, and

$$S_{i+1}\cong\lambda_i S_i, \tag{8}$$

where λ_i is the magnitude of the slope in the middle of the appropriate interval. Define λ by $\lambda^{n-1}=\lambda_2\lambda_3\cdots\lambda_n$. Yorke *et al.* [5] show then that the appropriate rescaling in the coordinate x and parameter μ to get the nth iterated map in the canonical form [Eq. (6)] is

$$v\sim(x-x_0)\lambda^{n-1}, \tag{9}$$

$$\nu\sim(\mu-\mu_0)\lambda^{2(n-1)}, \tag{10}$$

where μ_0 is the saddle-node parameter value at one end of the window and x_0 is the period-n point closest to 0 for $\mu=\mu_0$. In this canonical form the relevant coordinate length and parameter variation scales are of order one, so that

$$S_1^2\sim\lambda^{2(n-1)}\sim\Delta\mu. \tag{11}$$

Using the above, we estimate the average duration of a chaotic transient τ to be of the order of the inverse of the size of the largest immediate basin S_1. This is motivated by thinking of the dynamics under the nth iterated map as hopping around randomly in the interval $[\mu-\mu^2,\mu]$ with a probability of getting ''caught'' in the immediate basin proportional to its length,

$$\frac{1}{\tau}\sim S_1. \tag{12}$$

More precisely, if we uniformly sprinkle a very large number of points in the interval $[\mu-\mu^2,\mu]$ and we denote the num-

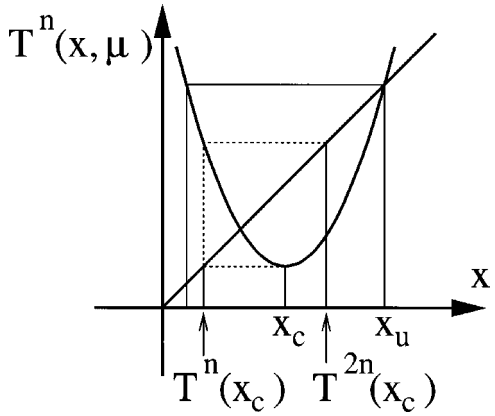

FIG. 2. $T^n(x,\mu)$ near the crisis for a period-n window.

ber of points that have not fallen in the immediate basin after t iterates by $N(t)$, then $N(t)$ will behave as

$$\frac{N(t)}{N(0)} \sim \exp\left(-\frac{t}{\tau}\right) \tag{13}$$

and this τ will be inversely proportional to the length of the largest basin S_1. Equations (11) and (12) imply that

$$\frac{1}{\tau} \sim (\Delta\mu)^{1/2}. \tag{14}$$

III. NUMERICAL VERIFICATION

We now wish to numerically test Eq. (14). We first find a large number of periodic windows with sizes varying over several orders of magnitudes. Our strategy is as follows. Using Newton's method, we find a value of μ for which the critical point is part of a period-n orbit (the orbit is then superstable) for some n:

$$T^n(0,\mu_{ss}) = 0. \tag{15}$$

Then we look for a slightly smaller μ value μ_{sn}, for which a saddle-node bifurcation occurs. At a saddle-node bifurcation, the map $T^n(x,y)$ has unit slope at its n fixed points,

$$T^n(x,\mu_{sn}) = x,$$

$$\frac{\partial}{\partial x} T^n(x,\mu_{sn}) = 1. \tag{16}$$

With our knowledge of μ_{sn} and μ_{ss} we can make an initial guess for the value of μ at the crisis μ_c at which the window ends. Based on the universal structure of high-period windows, we have $\mu_c \cong \mu_{sn} + 9(\mu_{ss} - \mu_{sn})$. Again applying Newton's method, we can greatly refine this initial guess using the crisis condition

$$T^{2n}(0,\mu_c) = T^{3n}(0,\mu_c). \tag{17}$$

To see why this is where the crisis occurs, consider Fig. 2, which is $T^n(x,\mu)$ near the critical point. The attractor will consist of n different pieces near the original period n orbit. The boundaries of the attractor near the critical point are

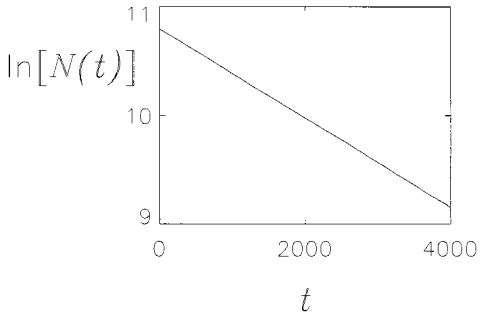

FIG. 3. Exponential decay of the number of points $N(t)$ that have not fallen in the immediate basin after t iterates.

$T^n(0,\mu)$ and $T^{2n}(0,\mu)$. Condition (17) means that $T^{2n}(0,\mu_c)$ is a fixed point of T^n, which implies that, at μ_c, the attractor collides with the unstable fixed point on the boundary and destroys the immediate basin.

Thus far, we have described how we numerically determine the window sizes $\Delta\mu$. Next we wish to determine the transient time τ at the superstable value μ_{ss}. (In Sec. IV we discuss the variation of τ with μ within a window.) Based upon the prediction for the size of the immediate basin [Eq. (11)], we look for an unstable fixed point x_u within $2.0(\Delta\mu)^{1/2}$ of the critical point and then determine the immediate basin at $[-x_u, x_u]$. Then we sprinkle a large number of points ($\sim 10^5$) in the interval $[T^2(0,\mu), T(0,\mu)]$ and compute for each one of these the number of iterates it takes for the orbit to first enter the immediate basin. Plotting the logarithm of the number of points that have not entered the immediate basin at time t versus t and fitting a straight line to the plotted data, we determine $1/\tau$ as the slope of this line, according to Eq. (13). Figure 3 shows such a plot for $\mu = 1.999\,64$ that lies in a period-ten window. Figure 4 shows results for the logarithm of $1/\tau$ versus the logarithm of $\Delta\mu$ for 186 different windows with periodicity up to 12. The resulting graph seems to be very well fitted by a straight line with slope 1/2 over seven decades, strongly confirming the prediction (14).

In order to show that the scaling law (14) does not depend on the particular form of the map, but only on the generic quadratic nature of the extremum, we also consider the cubic map

$$x \to T(x,\mu) = x^3 - 3\mu x. \tag{18}$$

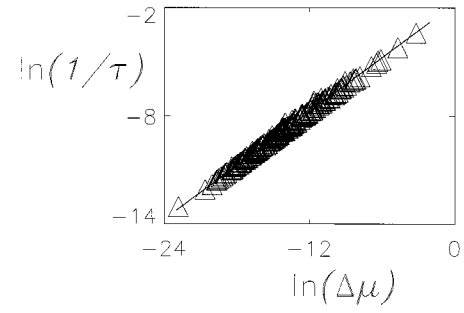

FIG. 4. Scaling of the decay time τ with the size of the window $\Delta\mu$ for the quadratic map $T(x,\mu) = \mu - x^2$.

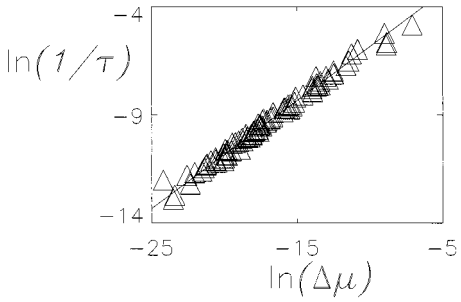

FIG. 5. Scaling of the decay time τ with the size of the window $\Delta\mu$ for the cubic map $T(x,\mu)=x^3-3x\mu$.

Because of the symmetry of this map, $T(-x,\mu)=-T(x,\mu)$ we will have coexisting attracting periodic orbits: If $x_1,x_2,\ldots,x_n$ forms an attracting periodic orbit, then so does $-x_1,-x_2,\ldots,-x_n$. Thus, to determine τ we check when randomly placed initial conditions first arrive at one of the two symmetrically placed immediate basins. The computation of periodic windows and transient times is analogous to the quadratic map. The resulting plot is shown in Fig. 5. Here again, the graph is very well fitted by a straight line with slope 1/2, as predicted by Eq. (14).

IV. PREDICTION FOR VARIATION OF TRANSIENT TIME WITHIN A SMALL WINDOW

When constructing Figs. 4 and 5, we computed the transient time at the superstable parameter value. The underlying assumption is that this transient time is somehow typical for all the transient times within the same window. We will argue here that this is indeed the case and that the variation of a normalized transient time with the variation of a (normalized) parameter in a window is given by a universal function.

We use a normalized parameter s for a window such that s is zero at the saddle-node bifurcation and one at the crisis:

$$s=\frac{\mu-\mu_{sn}}{\mu_c-\mu_{sn}}. \tag{19}$$

We then compute the transient time τ_{ss} at the superstable parameter value and normalize other computed values $\tau(s)$ with this one: $\tau(s)/\tau_{ss}$. We then claim that for typical small width windows $\tau(s)/\tau_{ss}$ approximately follows a universal curve and the agreement of $\tau(s)/\tau_{ss}$ with the universal curve becomes better as the window becomes smaller or, equivalently, as the period increases. This is again because universality means that the nth iterated map near an attracting period-n orbit can, under the proper rescaling, be brought in the canonical form (6) for which we know the saddle node and crisis occur at $\nu=0$ and $\nu=9/4$, respectively. For this form, we can explicitly determine, as a function of ν, the stable and unstable periodic points and therefore the size of the immediate basin near $x=0$. More precisely, since the saddle node and the crisis for Eq. (6) occur at $\nu=0$ and $\nu=9/4$, respectively, we have, for Eq. (6),

$$s=\frac{\nu}{9/4}. \tag{20}$$

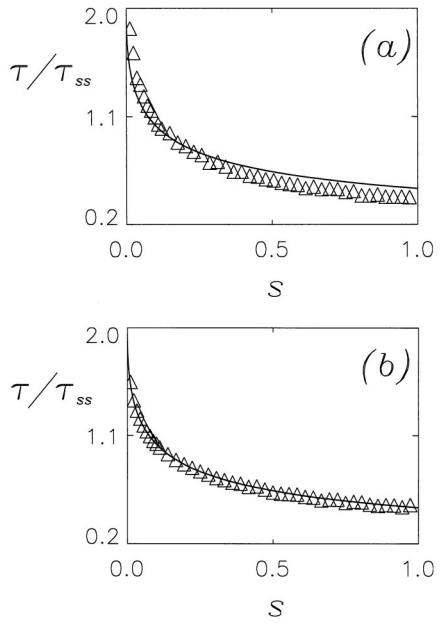

FIG. 6. Comparison between the prediction for the parameter dependence of transient time within a window (solid curve) and measured values (triangles) for the quadratic map for (a) a period-three window with size $\Delta\mu\approx 0.04$ and (b) a period-ten window with size $\Delta\mu\approx 1.58\times10^{-5}$.

As a function of ν, the fixed points of Eq. (6) are at $\pm(\nu)^{1/2}$, with $-(\nu)^{1/2}$ the stable one. This means that the basin will be enclosed by the points $v=(\nu)^{1/2}$ on the right and the negative solution of

$$v+v^2-\nu=\nu^{1/2}, \tag{21}$$

which is $-1-\nu^{1/2}$, on the left. Therefore, the size of the immediate basin is $1+2\nu^{1/2}$. If we divide by the size of the basin at the superstable value $\nu=1/4$ and use Eq. (12) for how the transient time scales with the immediate basin size, we obtain our universal result for the normalized decay time as a function of the normalized parameter s,

$$\frac{\tau(s)}{\tau_{ss}}=\frac{2}{1+3s^{1/2}}. \tag{22}$$

This predicts that the transient times at the saddle node and at the crisis are exactly twice and half as long as at the superstable parameter value. The longest transient time within one window is four times larger than the shortest.

Numerical evidence for this prediction is shown in Figs. 6(a) and 6(b). Figure 6(a) shows the normalized transient times (triangles) at different locations in the period-three window of the quadratic map near $\mu=1.75$, superimposed on the predicition (22) (solid line). The data and prediction roughly agree, but there is a significant deviation. However, the correspondence between the numerics and our prediction increases if we look at higher-period (narrower) windows. This is illustrated for a period-ten window of the quadratic map in Fig. 6(b). Again, this result holds for more general maps, and we show in Fig. 7 the corresponding graph for a period-nine window of the cubic map (18).

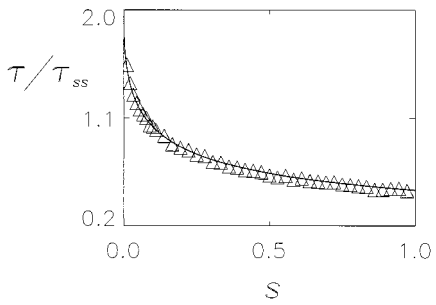

FIG. 7. Comparison between the prediction for the parameter dependence of transient time within a window and measured values for the cubic map for a period-nine window with size $\Delta\mu \approx 4.5\times10^{-8}$.

V. THEORY FOR TWO-DIMENSIONAL MAPS

Equation (14) was derived and numerically verified for one-dimensional maps. In order to investigate what happens for a two-dimensional invertible map we consider the Hénon map,

$$(x,y)\rightarrow(a-x^2+by,x), \tag{23}$$

which contains the one-dimensional quadratic map (5) when we set $b=0$. We study the effect of perturbing the one-dimensional case by using small-b values.

Consider parameter values (a,b) with $0<b\ll1$, for which we have an attracting period-n orbit [note that for Eq. (23) $y_n=x_{n-1}$],

$$(x_1,x_n),(x_2,x_1),\ldots,(x_n,x_{n-1}), \tag{24}$$

which lies in a periodic window $(a_0<a<a_c,b)$, where the saddle-node bifurcation and the crisis occur at $a=a_0$ and $a=a_c$, respectively. We assume that for $1\gg b>0$, a typical period-n window is close to a corresponding period-n window of the $b=0$ map. We denote a period-n window of the $b=0$ map by $a_0'<a'<a_c'$. We further assume that there are two period-n periodic orbits in the $b\neq0$ map window that are continuations of the two period-n periodic orbits in the $b=0$ window. Denote by a_{ss}' the superstable value for the period-n attractor in the $b=0$ window and for a_{ss}' we have a periodic orbit of the $b=0$ map

$$(0,x_n'),(x_2',0),\ldots,(x_n',x_{n-1}'). \tag{25}$$

Also, denote the closest unstable period-n point for $(x_2',0)$ by (x_u',y_u') (so that in one dimension the immediate basin is formed by $[-y_u',y_u']$) and the corresponding point for (a_{ss},b) by (x_u,y_u). If b is very small, we have that the periodic orbit for (a_{ss},b) is only a slight perturbation of the periodic orbit for $(a_{ss}',0)$:

$$x_1\cong0,\quad x_2\cong x_2',\ldots,\quad x_n\cong x_n' \tag{26}$$

and, similarly,

$$x_u\cong x_u',\quad y_u\cong y_u'. \tag{27}$$

For $b=0$ the entire square $[-2,2]\times[-2,2]$ will be projected after one iterate onto the parabola $x=a'-y^2$. The stable manifolds of fixed points or periodic points on this parabola are determined by vertical lines $x=$const. This is depicted in Fig. 8(a). Now consider Fig. 8(b), which shows the attracting point (x_2,x_1) in the periodic orbit, the closest unstable period-n point (x_u,y_u), and its stable and unstable manifold. Also drawn in this picture are the parabolas $x=a-y^2+2b$ and $x=a-y^2-2b$. After one iterate of Eq. (23), the square $[-2,2]\times[-2,2]$ will be mapped between these two parabolas. Now consider a parameter value a, just smaller than a_0, for which there is a chaotic attractor that lies between the parabolas of Fig. 8(b). We depict this attractor schematically in Fig. 8(c).

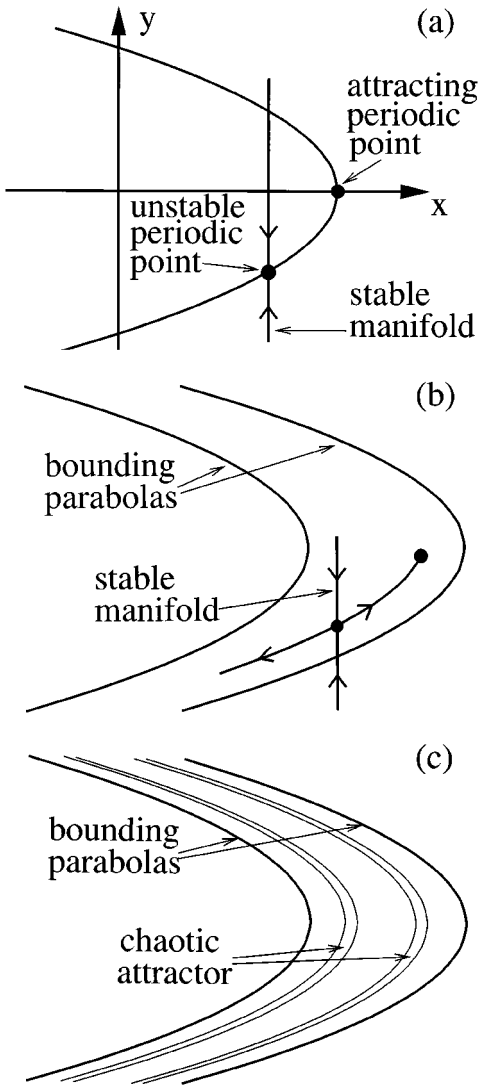

FIG. 8. (a) Attracting periodic point and closest nonattracting periodic point for $b=0$. (b) Stable periodic point and closest unstable periodic point with its stable and unstable manifold for $b\neq0$. (c) Chaotic attractor bounded by the parabolas $x=a-y^2+2b$ and $x=a-y^2-2b$.

For values of a in the periodic window, the forward iterates of points in the square $[-2,2]\times[-2,2]$ will exhibit transient behavior similar to that of the chaotic attractor for a while before being attracted to the stable periodic orbit. During its transient behavior, as soon as an orbit falls to the right of the stable manifold of the unstable point (x_u,y_u), it will converge to the attracting periodic orbit. Therefore, we can

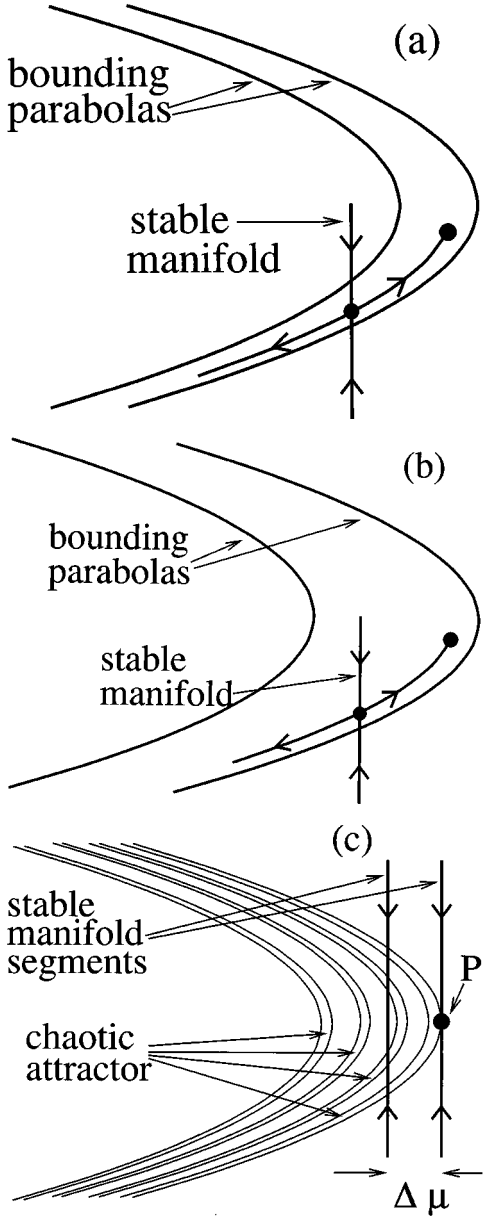

FIG. 9. (a) Windows for which $\Delta\mu > b$ exhibit one-dimensional scaling behavior. (b) When $\Delta\mu < b$ the scaling becomes $1/\tau \sim (\Delta\mu)^{d-1/2}$. (c) Construction for estimating the measure of the immediate basin.

consider the region to the right of this stable manifold and to the left of the parabola $x = a - y^2 + 2b$ to be the immediate basin.

The width of the attractor transverse to its striations is of the order of b (the absolute value of the Jacobian determinant of the map), as is the separation between the two parabolas of Fig. 8(b). From Eqs. (26) and (27) and the form of the Hénon map (23), it can be seen that the x and y coordinates of the stable and unstable orbits differ by numbers of the order of S_1 and S_1^2, respectively, where S_1 is the length of the immediate basin in one dimension ($b = 0$). Therefore, depending on the relative size of S_1^2 ($\sim\Delta\mu$) and b (separation of the parabolas), one can have one of the two situations depicted in Figs. 9(a) and 9(b). In Fig. 9(a), b is smaller than $\Delta\mu$ and therefore the probability of falling to the right of the stable manifold of the unstable periodic point is essentially the same as that of falling in the immediate basin in the one-dimensional case.

We now wish to obtain the scaling of τ^{-1} with $\Delta\mu$ for the case $\Delta\mu < b$. That is, we desire an estimate of the probability that a given iterate of the chaotic transient lands in the immediate basin region shown in Fig. 9(b). As previously shown, this region has a horizontal width of the order of $\Delta\mu$. Consider the attractor that exists before (but not too close to) the beginning of the window. We estimate τ^{-1} to scale as the attractor measure contained within a region bounded by the outer (rightmost) edge of the attractor and a stable manifold segment horizontally displaced from the rightmost point P on the attractor by the distance $\Delta\mu$ [see Fig. 9(c)]. The measure of this region can be estimated for small $\Delta\mu$ as follows. The measure of a box of side ϵ containing P scales as ϵ^d for small ϵ, where d denotes the pointwise dimension of the attractor at the point P. Now take $\epsilon = \Delta\mu$ and cover the immediate basin region shown in Fig. 9(c) with boxes. The quadratic nature of the tangency of the unstable manifold with the stable manifold segment through the point P implies that the vertical extent of the immediate basin region in Fig. 9(c) is of the order of $(\Delta\mu)^{1/2}$. The measure of an ϵ box is $(\Delta\mu)^d$ for $\epsilon = \Delta\mu$, and we need of the order of $(\Delta\mu)^{1/2}/\Delta\mu = (\Delta\mu)^{-1/2}$ boxes to cover the immediate basin region. Thus the measure of the immediate basin region is of the order of $(\Delta\mu)^d \times (\Delta\mu)^{-1/2} = (\Delta\mu)^{d-1/2}$. Hence we obtain

$$\frac{1}{\tau} \sim (\Delta\mu)^{d-1/2} \tag{28}$$

for $\Delta\mu < b$.

VI. NUMERICAL COMPARISON FOR THE HÉNON MAP

To numerically test Eq. (28) at different b values, we first determine many windows and find the transient time at a parameter value of one-ninth of the way through the window (analogous to superstable value for $b = 0$). By constructing a $\ln(1/\tau)$ versus $\ln(\Delta\mu)$ graph, as in Figs. 4 and 5, we will infer the slope and compare that with the prediction (28).

To determine windows, we start with the windows that we found for the $b = 0$ case, as described in Sec. III. We find the periodic orbit and then look for $(a, b \neq 0)$ values with a periodic orbit close to the original one. We then repeat this step for larger-b values starting with the periodic orbit at the intermediate-b value. In this way, we attempt to track the $b = 0$ windows to large-b values. In this way we are able to find a large number of windows, with widths as small as 10^{-9}, up to $b = 10^{-2}$. A brute force method, checking for periodicity on a lattice of a points at $b = 0.3$, is also applied to find windows as small as 10^{-6}.

To find transient times, consider the Jacobian matrix $\boldsymbol{DT}^n$ at one of the points $\boldsymbol{x}_p$ on the stable period-n orbit. This matrix has two eigenvalues that are smaller than one in absolute value and two eigenvectors $\boldsymbol{e}_1$ and $\boldsymbol{e}_2$ (which in general are not orthogonal). Within the linear approximation (i.e., for small enough K), T^n will map the ellipse $\boldsymbol{x}_p + K[\cos(\theta)\boldsymbol{e}_1 + \sin(\theta)\boldsymbol{e}_2]$ for $0 \leq \theta < 2\pi$, within itself. There is a largest value of K (denoted K_m) such that the ellipse nonlinearly maps to within itself. Choosing $K < K_m$,

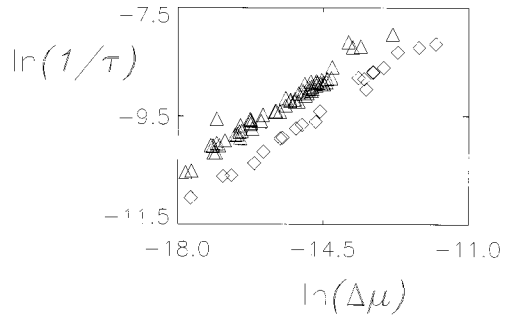

FIG. 10. Dependence of the scaling law in two dimensions on the period. The plot of $\ln(1/\tau)$ versus $\ln(\Delta\mu)$ for windows of period 17 (triangles) appears to lie on a line parallel with the plot for windows of period 10 (diamonds).

we consider the corresponding ellipse to be the immediate basin and determine τ as in the one-dimensional case.

Alternatively, one can take a large number of initial conditions and determine how long it takes them to come within a distance ϵ of one of the points on the period-n orbit. Then, again by making a graph of $\ln[N(t)]$ versus t, we determine the inverse of the slope of this graph to be τ_ϵ. We expect that as we decrease ϵ starting at some initial value, τ_ϵ will continue to increase until the circle with radius ϵ fits into the immediate basin. When continuing to decrease ϵ further from this value onward, τ_ϵ will essentially remain constant as the convergence toward the periodic point will happen extremely fast once inside the immediate basin. This is indeed what we observe numerically: Decreasing ϵ will increase τ_ϵ up to some point where τ_ϵ levels off and remains approximately constant. This we call the transient time τ and compare it with the τ obtained with the previously described method. For the parameter values we worked with, this method and the ellipse method gave the same values for the transient times.

Another difference with the one-dimensional case is evident from the plot in Fig. 10. This plot shows results for τ as a function of $\Delta\mu$ for windows for $b=10^{-4}$, where period-17 windows are indicated with triangles and period-10 windows with diamonds. There is a clear separation between the data for the two periods. Evidently windows with a fixed period seem to satisfy

$$\frac{1}{\tau}=C(\Delta\mu)^{\alpha}, \tag{29}$$

but there is a dependence of the constant C on the period. For the different b values and periods that we looked at, C is monotonically increasing as a function of the period.

Figure 11 shows a plot of the exponent α versus b, where α is obtained from the slope of straight lines fitted to plots such as in Fig. 10. The error bars in Fig. 11 indicate the goodness of the fitted straight lines. For the three points to the left of the dotted line (at $b=10^{-6}$, 10^{-5}, and 10^{-4}), enough windows were found that we were able to determine a slope for six individual periods and then average. However, for the three points to the right of the dotted line (at $b=10^{-3}$, 10^{-2}, and 0.3) the windows from four periods (10, 11, 12, and 13) are taken together, and we fit a single line through these points. This was done because the number of

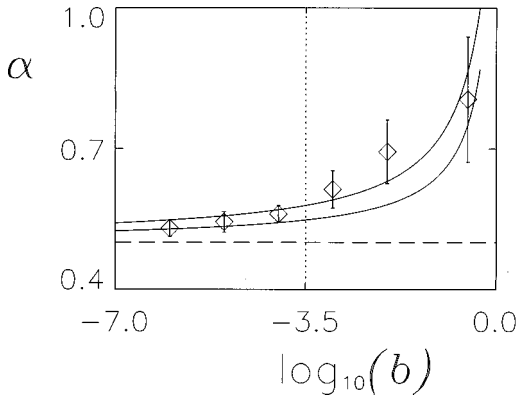

FIG. 11. Data for the scaling exponent α for different values of the Jacobian determinant. The two solid lines are predictions for the exponent α based on the Kaplan-Yorke prediction for the dimension with $\lambda=1.5$ (lower line) and $\lambda=2.0$ (upper line). The dashed line gives the exponent for the one-dimensional scaling. The error bars on the values for $b=10^{-3}, 10^{-2}$, and 0.3 are larger because fewer windows are obtained.

windows was not large enough to make a fit individually for each period. For all six data points, only windows with $\Delta\mu<b/5$ were used. Smaller-b values (10^{-7} and 10^{-8}) do not give reliable results for the slope because so few windows are found that the transition from fitting a slope with windows for which $\Delta\mu<b/5$ to only retaining the ones with $\Delta\mu<b$ gives a large variation in the value of the slope.

The two solid lines in Fig. 11 indicate the predictions for the value of the exponent as a function of b according to Eq. (28). If we estimate the pointwise dimension d at P in Fig. 9(c) using the information dimension of the attractor, we can use the Kaplan-Yorke formula to estimate d. Let $h_1>0>h_2$ be the two Lyapunov exponents on the attractor. Since the Jacobian determinant (i.e., $-b$) of our map is constant, we have that $h_1+h_2=\ln(b)$. The Kaplan-Yorke formula then yields

$$d=1+\frac{h_1}{|h_2|}=1+\frac{\ln(\lambda)}{\ln(\lambda)-\ln(b)}. \tag{30}$$

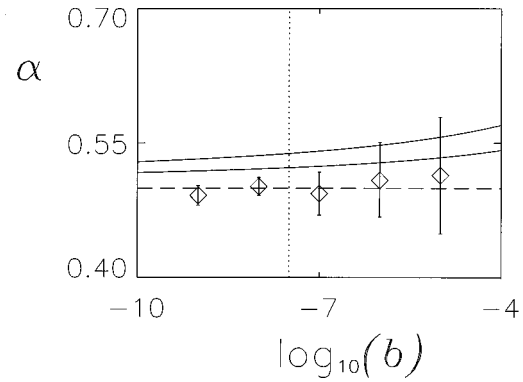

FIG. 12. One-dimensional scaling regime for two-dimensional maps: windows that are larger in size than the Jacobian determinant. The solid lines represent the predictions for the scaling of windows larger than the Jacobian and the dashed line represents the one-dimensional prediction. Especially for the smaller values of b, the scaling is like in the one-dimensional case, as expected.

According to [7], typical values for λ can be expected to be around $1.5<\lambda<2.0$ for small-b values. Therefore, in Fig. 11 the two solid lines represent predictions for the exponent $d-1/2$, with an estimate for d obtained by using two extreme values of $\lambda=1.5$ and $\lambda=2.0$ in Eq. (30). Remember that for one-dimensional maps, this exponent would be 0.5. For comparison, this line $y=0.5$ is also included in this figure as a dashed line.

One can see that there is qualitative agreement of the prediction with the data (the exponent is definitely different from the one-dimensional case and is an increasing function of b), but the agreement of the numerical values is not good enough to definitely confirm the conjecture (28). Detailed agreement is also hard to expect because windows that are near chaotic attractors with different dimensions are all used in the same graph to fit one slope.

Finally, in Fig. 12 we show the results for the windows that satisfy $\Delta\mu>5b$ for five different b values (from 10^{-9} to 10^{-5}). Here again, for the points to the left of the dotted line, four different periods were averaged, whereas for the points to the right of this line, just one fit was obtained by lumping all data for the different periods together (because not enough windows were obtained per period for an individual fit). The best possible values all lie close to the predicted value of 0.5 (the one-dimensional scaling, represented by the dashed line), but the error bars for the larger-b values are too large for the measured values to be bounded away from the prediction for the $\Delta\mu\ll b$ scaling (solid lines).

VII. CONCLUSION

For one-dimensional maps, we derived a scaling law for the dependence of transient times in periodic windows on the size of those windows. Numerically, this law was shown to be satisfied quite accurately, independent of the specific form of the map. The same scaling law holds for two-dimensional maps only if the Jacobian determinant of the map is very small. We gave a heuristic argument for a scaling law that holds more generally and provided some numerical evidence for the existence of these different scaling regimes in two dimensions. Qualitative features of the conjecture for scaling in two dimensions were confirmed by a numerical experiment.

ACKNOWLEDGMENTS

This work was supported by the Office of Naval Research and by the U.S. Department of Energy. The numerical computations reported in this paper were supported in part by a grant from the W. M. Keck Foundation.

[1] See, e.g., E. Ott, *Chaos in Dynamical Systems* (Cambridge University Press, Cambridge, 1993), and relevant references therein.
[2] C. Grebogi, E. Ott, and J. A. Yorke, Physica D **7**, 181 (1983); Phys. Rev. Lett. **48**, 1507 (1982).
[3] J. Graczyk and G. Świątek, Ann. Math. (to be published).
[4] M. V. Jacobson, Commun. Math. Phys. **81**, 39 (1981).
[5] J. A. Yorke, C. Grebogi, E. Ott, and L. Tedeschini-Lalli, Phys. Rev. Lett. **54**, 1095 (1985); B. R. Hunt, J. A. C. Gallas, C. Grebogi, J. Yorke, and H. Koçak (unpublished).
[6] J. Yorke and E. Yorke, J. Stat. Phys. **21**, 263 (1979).
[7] B. R. Hunt and E. Ott, J. Phys. A **30**, 7067 (1997).